ADVANCED MATERIALS INTERFACES

www.advmatinterfaces.de

Creating Superhydrophobic Polymer Surfaces with Superstrong Resistance to Harsh Cleaning and Mechanical Abrasion Fabricated by Scalable One-Step Thermal-Imprinting

*Zhibing Zhan, Zihao Li, Xiaoyun Li, Erik Garcell, Subhash Singh, Mohamed ElKabbash, and Chunlei Guo**

In this work, a scalable thermal imprinting method that allows to directly fabricate superhydrophobic polymer surfaces with superstrong resistance to harsh cleaning and mechanical abrasion is reported. A titanium (Ti) mold is produced by femtosecond laser processing to possess a hierarchical micro- and nanoscale pattern. Through thermal imprinting, this hierarchical pattern onto poly(propylene) sheets is able to be accurately reproduced, rending the polymer surface superhydrophobic. The imprinting method employed uses an aqueous ethanol solution of stearic acid to assist demolding, and periodically uses xylene to limit mold contamination and restore the mold to excellent condition for further imprinting. These strategies allow to repeatedly use the mold over 50 times without degradation. A range of durability tests are further performed, and showed that the produced suprehydrophobility on the poly(propylene) sheets exhibit excellent durability, withstanding brush washing, ultrasound cleaning, and sandpaper abrasion. The reported method can also be used to fabricate superhydrophobic surfaces of various thermoplastics that are broadly utilized in daily life.

1. Introduction

A superhydrophobic surface (SHS) is normally defined as a surface with a water contact angle larger than 150° and sliding angle less than 10°.[1] SHSs usually come from the effects of a range of hierarchical surface micro- or nanostructures and nonpolar surface chemistry.[1e,2] As a result, SHSs repel water and stay dry and clean.[1c,3] Due to this unique property, SHSs have attracted a great amount of interest and have potential applications in self-cleaning, anti-icing/fogging, anticorrosion, oil/water separation, and water/fog harvest.[1a,4] For these surface applications, superhydrophobic (SH) effects are particularly useful on polymers, because polymers are low-cost, lightweight, and corrosion-resistant.[4a,5] Poly(prophlene) (PP) is the second-most widely produced synthetic plastics, and it has a wide range of applications in industry as well as in household activities such as home appliances, automotive, and package films.[5b,c] Not having polar groups in its chemical composition, PP is intrinsically hydrophobic with a contact angle of about 100°.[5a,b] In 2003, Erbil et al. reported an approach of fabricating SHSs with PP via controlling the phase separation process by adding proper amounts of nonsolvents.[5a] This solution casting technique was later followed extensively, in which a PP bulk is dissolved in p-xylene liquid at a relatively high temperature, then the suspension containing the etched PP particles is casted onto substrates to form an SH layer.[5b,c,6] Although this casting method is effective to fabricate PP SHSs, the adhesion of casted SH layers to various underlying substrates should be considered.[5a,7] The weak adhesion with time may result in the peeling of the SH layers, which seriously affects the applications of the SHS.

Different from coating or casting methods, thermal imprinting can pattern various substrates to form micro- and nanostructured textures on their surfaces directly.[8] With the advantages of low cost, mass-production, and flexibility in material choice, thermal imprinting has been widely used to duplicate SH structures on polymers or even metals.[8c,d,9] However, the mechanical durability and washability of the produced structures and the associated SHSs have not been tested extensively. In fact, for practical use of SHSs, mechanical durability is always a major concern, as mechanical wear and abrasion can result in the loss of superhydrophobicity.[1c,3a] The washable property of SHSs is also essential to many practical applications of SHSs, as contamination and fouling of SHSs are often unavoidable, such as in water–oil separation.[4f,10] During thermal imprinting, the repeated use of the mold is a key factor, which determines the cost and efficiency of the imprinting process. So far, few work reported on the strategy of extending the lifespan of molds.

Dr. Z. Zhan, Z. Li, X. Li, E. Garcell, Dr. S. Singh, Dr. M. ElKabbash, Prof. C. Guo
The Institute of Optics
University of Rochester
Rochester, NY 14627, USA
E-mail: guo@optics.rochester.edu
Dr. S. Singh, Prof. C. Guo
Changchun Institute of Optics
Fine Mechanics, and Physics
Changchun 130033, China

The ORCID identification number(s) for the author(s) of this article can be found under https://doi.org/10.1002/admi.201900240.

DOI: 10.1002/admi.201900240

In this work, we reported on a method that can directly convert a normal PP surface to an SHS just through a one-step thermal-imprinting approach. The titanium (Ti) molds for imprinting are fabricated by our femtosecond (fs) laser processing method, whose surface consists of hierarchical micro- and nanostructures. Under suitable thermal imprinting parameters, the PP samples exhibit outstanding superhydrophobicity. By using aqueous ethanol solution of stearic acid and xylene liquid to assist in the demolding process and to remove the PP particles remaining on Ti mold surface, respectively, our strategy guaranteed the repeatability of the Ti mold. This method is fast, easy, and cost-effective, and can be used to fabricate SHSs of various thermoplastics that are broadly utilized in our daily life. Furthermore, the imprinted polymer SHSs show outstanding washable property and mechanical durability, which should have important significance for the fabrication of plastic SHSs and their applications.

2. Results and Discussion

A Ti plate, ablated by fs laser pulses, was used as the mold in the process of thermal imprinting. Commercial PP with thicknesses of 1.6 mm were cut to ≈35 mm squared sheets and used as the imprinting materials, which are shown in **Figure 1**. The Ti plate before and after fs laser treatment is shown in Figure 1a,b, respectively. As can be seen, the fs laser processing changes the surface color and morphology, and the treated surface appears pitch black with near-unity optical absorption. The 3D surface profile of the Ti mold shown in Figure 1c demonstrates that the surface has rough microstructured morphology. Typical PP sheets without and with thermal imprinting are show in Figure 1d,e. Laser microscope image of the 3D profile of the PP surface after thermal imprinting is shown in Figure 1f. It is very clear that the PP surface replicated the negative structure of the Ti mold (Figure 1c,f). The water drops on PP surfaces with and without thermal imprinting treatment (insets in Figure 1d,e) confirm that our thermal imprinting changed the hydrophobic PP surface to SHS, as the contact angles increase from about 102° to more than 150°. Due to the excellent superhydrophobicity, when a drop of water is released and falls towards the SHS, the water droplet is repelled by the SHS to such a degree that it bounces off the surface, lands again due to gravity, and bounces again and off the surface, as shown in Movie S1 of the Supporting Information.

To check the fidelity between the Ti mold surface and PP surface after thermal imprinting, we randomly chose two cross-sections, one from the Ti mold and one from an imprinted PP surface, and compared the height variations of these two surfaces. Laser microscopy images of the top-view and a cross-section showing the height variation for Ti mold and PP sample are shown in **Figure 2**a,b, respectively. The height variation of PP sample (red curve in Figure 2c) is obtained by inverting the cross-section of the imprinted PP (Figure 2b), in order to compare with that of Ti mold (black curve in Figure 2c that originates from Figure 2a directly). The similar curves of the height

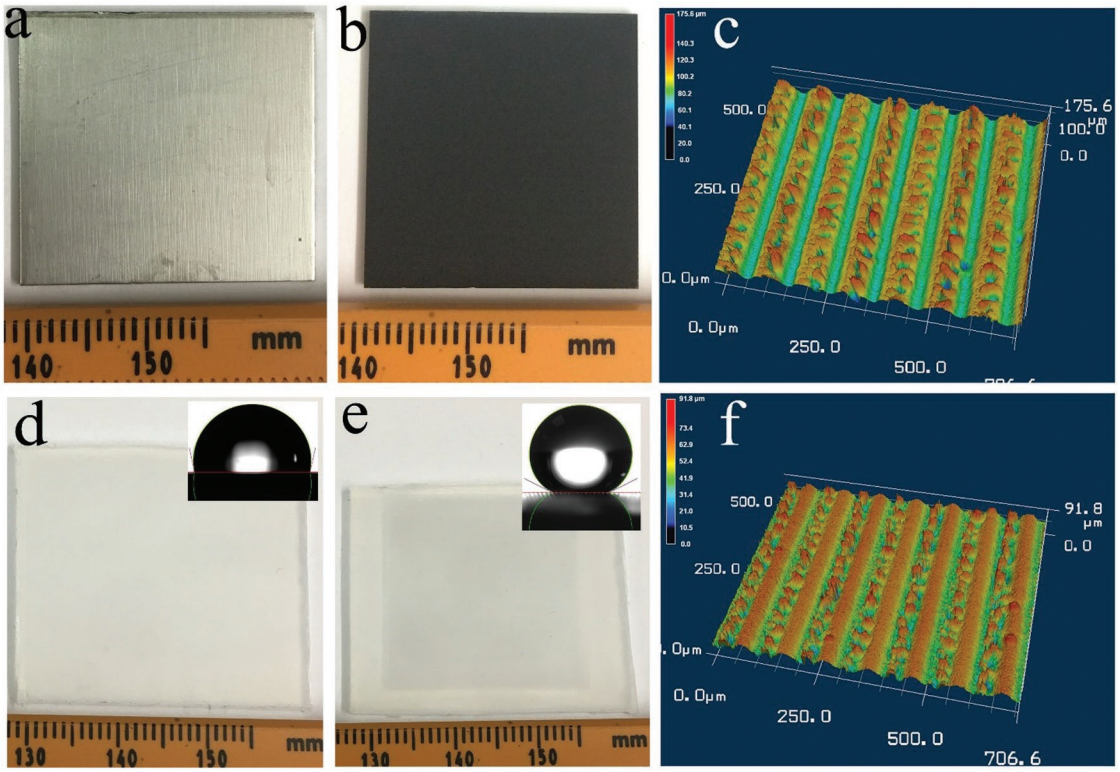

Figure 1. Photos of a Ti plate a) before and b) after fs laser treatment, laser microscope of 3D surface profile of c) the Ti mold; and photos of PP sheets d) without and e) after thermal imprinting, laser microscope of 3D surface profile of the PP sheet f) after thermal imprinting. The insets in (d) and (e) are typical images of water droplets on corresponding PP surfaces.

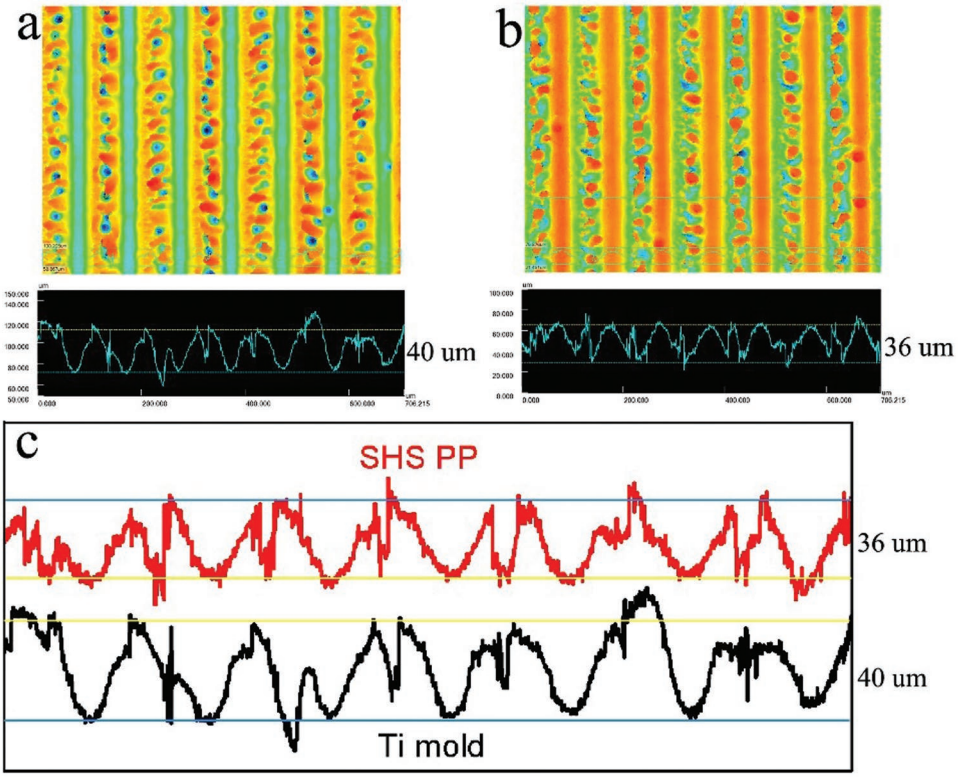

Figure 2. a,b) Laser microscopy images of the top-view and a cross section showing the height variation for Ti mold (a) and PP sample after thermal imprinting (b). c) The height variation of imprinted PP sample (red curve) that is obtained by inverting the cross-section of PP sample (b), and Ti mold (black curve) that originates from Ti surface directly (a).

variations demonstrate that our thermal imprinting method precisely replicated the negative structure of the Ti mold on PP surface. The average height of thermal imprinted ridges on PP surface (about 36 μm) reach about 90% of the average depth of the grooves on the Ti mold (about 40 μm), as shown in Figure 2c.

In order to optimize the experimental parameters for the fabrication of PP SHSs, we carried out the thermal imprinting process under a series of temperature and pressure and measured the contact angles of all imprinted PP samples. The experimental results are shown in **Table 1**. As shown, the contact angle increases with the increasing of the imprinted temperature and pressure, as high temperature and pressure are advantageous to replicate the structure of the Ti mold on PP surface. However, high temperature and pressure are disadvantageous for the Ti mold and PP samples, as Ti mold and PP samples are easily to be damaged during the thermal imprinting and the further demolding processes under this harsh situation. For the temperature below 100 °C, it is rather hard to fabricate the PP SHS by thermal imprinting method, as the PP sheet is still hard at this temperature and difficult to be imprinted, which can be seen by the laser microscope of the PP sample imprinted under the temperature of 75 °C and pressure of 15 MPa (Figure S1, Supporting Information). By comparing the obtained values of the contact angle, we finally chose a temperature of 115 °C and pressure of 15 MPa as the optimized parameters for our thermal imprinting process, because higher temperatures and pressures did not result in stronger superhydrophobicity (Table 1) and instead result in the warpage or distortion of PP sheets after thermal imprinting.[11] In addition, to obtain superhydrophobicity, the period of the imprinted structures on PP surfaces in our experiment should be no larger than ≈100 μm (see explain in Figure S2, Supporting Information) and the depth of the structures no shallower than about 30 μm (Figure 2; Figure S1, Supporting Information).

Table 1. Measured contact angles as the function of the temperature (*T*) and pressure (*P*) during the thermal imprinting process for PP SHSs.

P \ *T*	75 °C	100 °C	115 °C	130 °C
5 MPa	117°	120°	137°	144°
10 MPa	125°	136°	142°	148°
15 MPa	128°	146°	154°	155°
20 MPa	131°	148°	152°	153°

The initial five PP samples imprinted by the Ti mold are shown in **Figure 3**a. Obviously, the first PP sample looks darker than the other samples. This is due to the transform of the nano/microparticles from the surface of the Ti mold during the first thermal imprinting process, which can be confirmed by the SEM images of the mold surfaces before (Figure 3b,c) and after (Figure 3d,e) this first imprinting. The fs laser treatment will result in some deposits on the laser induced period structures,[12] as shown in Figure 3b,c. These deposit particles

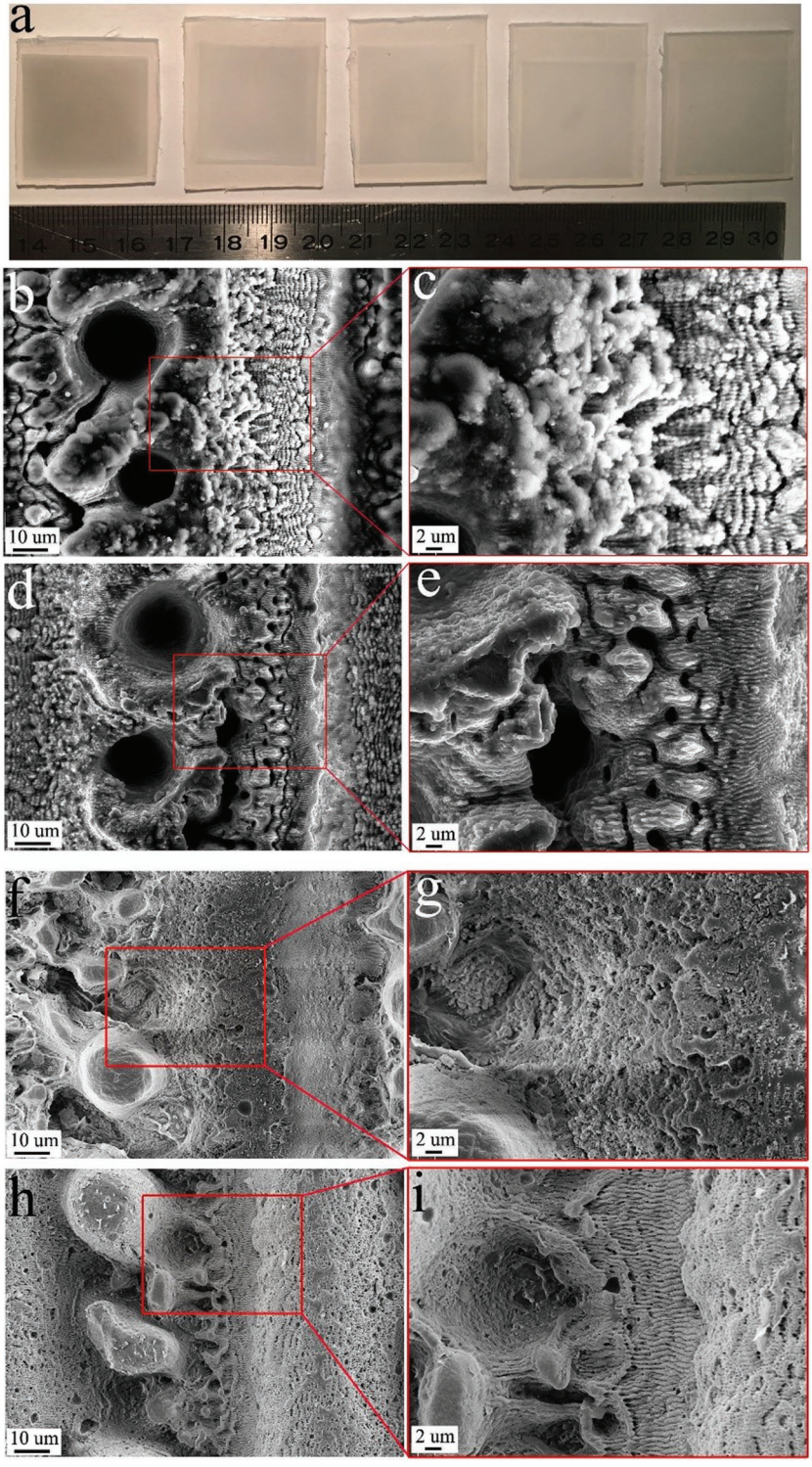

Figure 3. a) Photo of the initial five PP samples, and SEM images of Ti mold surfaces b,c) before and d,e) after the first time of thermal imprinting, and SEM images of f,g) the first and h,i) second PP samples.

can be easily transferred to the PP surface during the first thermal imprinting process. As shown in Figure 3d,e, only these deposits are lost from the surface of the Ti mold after the first time of the thermal imprinting, while the rest of the laser induced micro/nanostructures will remain. Figure 3f–i shows the surface morphologies of the first (Figure 3f,g) and second (Figure 3h,i) PP samples. After removal of the deposits from Ti mold surface, the remaining surface micro/nanostructures are imprinted on the PP surface, which can be observed clearly (Figure 3h,i). More SEM images to show the morphology change of the surfaces on the Ti mold and PP samples can be found in Figures S3 and S4 of the Supporting Information. The EDX results of Ti surfaces before and after fs laser processing demonstrate that the laser ablation in air results in oxidation of the Ti surface, as shown in Figure S5 of the Supporting Information. It should be noted that this first transform of these deposit particles from the Ti mold does not affect the subsequent thermal imprinting process, as shown in our results that the imprinting performance persists over 50 times. We will show in the following part that all the thermal-imprinted PP samples (including the first one with transformed deposit particles) exhibit superhydrophobicity with high contact angle and low sliding angle.

To check superhydrophobicity, we measured the contact angles and sliding angles of all the PP samples after thermal imprinting. For contact angle measurement, we measured five points which are located at the center and at the four corners on the PP surface, as shown in **Figure 4**a (inset). From the measured results, we can find that the highest contact angle is about 163° and the lowest one is ≈142°, as shown in Figure S6 of the Supporting Information. Based on the results, we obtained the average contact angle for every PP sample, which are all about 150°, as shown in Figure 4a. The sliding angles are about 4°–7°. We also calculated the contact angle hysteresis,[13] which is about 7°, as shown in Figure S7 of the Supporting Information. These results mean that the thermal imprinted PP samples fulfilled the definition of SHSs. Also, there is no obvious differences of contact angle, contact angle hysteresis and sliding angle that are parallel and perpendicular to the grating, which demonstrated that the superhydrophobicity of the polymer surface at here is isotropic, due to enough roughness of the thermal imprinted surface.[14] All the measured RMS roughness (Rq) of the thermal imprinted PP surfaces are larger than 12 μm, as shown in Figure S8 of the Supporting Information. We also measured the contact angle of the untreated PP sheet, which is about

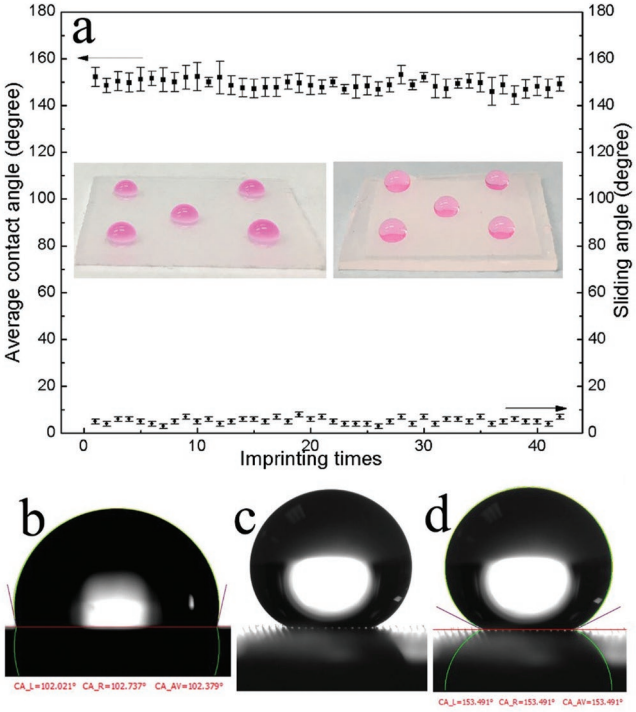

Figure 4. a) Average contact angles and sliding angles of all the 42 PP SHSs (contact angles were measured at five typical positions which are located at the center and at four corners of the sample, as shown inset). b–d) Images of a water droplet on a normal PP surface (b), the thermal imprinted PP surface before (c) and after (d) automatic fitting by software of the contact angle meter (CAST 3.0).

102°. Images of water droplets on a processed and unprocessed PP surface are shown in Figure 4b–d. From Figure 4c, showing a water droplet on an imprinted PP surface, we can see the small air cushion between the PP surface and the water droplet clearly (small white points at the interface). The air cushion is trapped in the nano- and microscale textures on the thermal imprinted PP surface, which is the origin of the sup erhydrophobicity.[1c,5a,15] As comparing, the image of a water droplet on an unprocessed PP surface shown in Figure 4b shows that there is no trapped cushion and the measured contact angle is only about 102°, due to no micro/nanoscale surface textures.

As described in Experimental Section, every time before the thermal imprinting, we immersed the Ti mold into an aqueous ethanol solution of stearic acid (0.1 M) for 3 min to assist in the following demolding process. This strategy is critical for the repeated use of our Ti mold. To compare, the same thermal imprinting process was performed by using a Ti mold without immersing it into the solution of stearic acid. The images of this Ti mold before and after the first thermal imprinting, and some PP samples are shown in Figure S9 of the Supporting Information. After the first time of thermal imprinting, we can find that a small area on the surface of the Ti mold lost the original black color (Figure S9c, Supporting Information), which means that the formed micro- and nanostructures on this small part is damaged. This damaged area affects subsequent thermal imprinting, which can easily be found on the surfaces of second and third PP samples (see Figure S9e,f, Supporting Information). It should be noted that the first PP sample shown here is also darker than others (Figure S9d, Supporting Information), due to the transfer of the micro- and nanostructures from the surface of the Ti mold to the first PP sample as described above. With the stearic acid solution to assist in demolding process, the Ti mold does not show any damage even through more than 40 times of thermal imprinting, which confirmed that our strategy, using stearic acid solution to assist in the following demolding process, can greatly extend the life of the imprinting mold. Therefore, this strategy has important significance for the large production of PP SHSs.

Although an aqueous ethanol solution of stearic acid was used every time before thermal imprinting to assist the demolding process, the deposition of PP particles on the Ti mold surface is still difficult to avoid. Especially, when the thermal imprinting process is carried out a large number of times. As shown in **Figure 5**a,a′, the surface of the Ti mold is obviously contaminated by PP particles after 42 thermal imprinting runs. Many small PP particles, several micrometers in size, are left on the Ti mold surface after demolding, and some of the large particles can be observed by the naked eye, as shown in Figure 5a′. These remaining PP particles may degrade the effect of the thermal imprinting after large number times of thermal imprinting, as shown in Figure S10 of the Supporting Information. It is luck that this contamination of PP particles can be removed by xylene solution at 120 °C.[5a,b] As shown in Figure 5b,b′, the surface of the Ti mold is cleaned through immersing it into xylene solution for 90 min. After this cleaning, we carried out thermal imprinting ten times by using this now cleaned Ti mold. The measured contact angle result shows that cleaning the Ti mold has no effect on the superhydrophobicity of PP surface, as shown in Figure S11 of the Supporting Information.

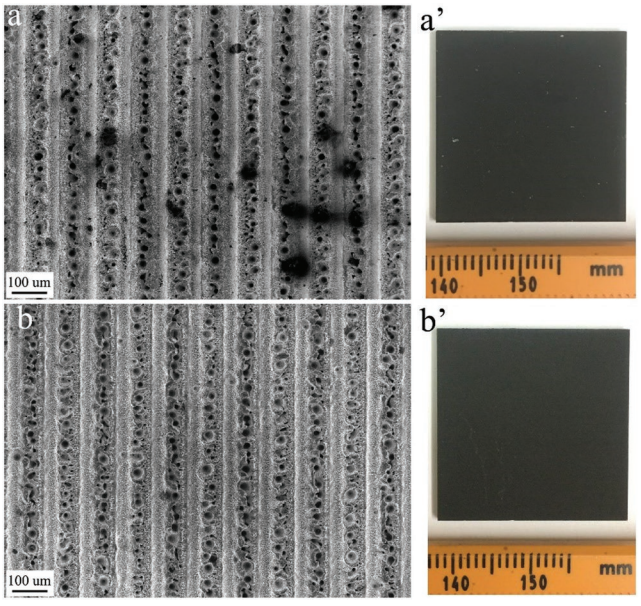

Figure 5. SEM images and sample photos of the Ti mold after 42 times of thermal imprinting a,a′) before and b,b′) after cleaning by xylene liquid at 120 °C for 90 min.

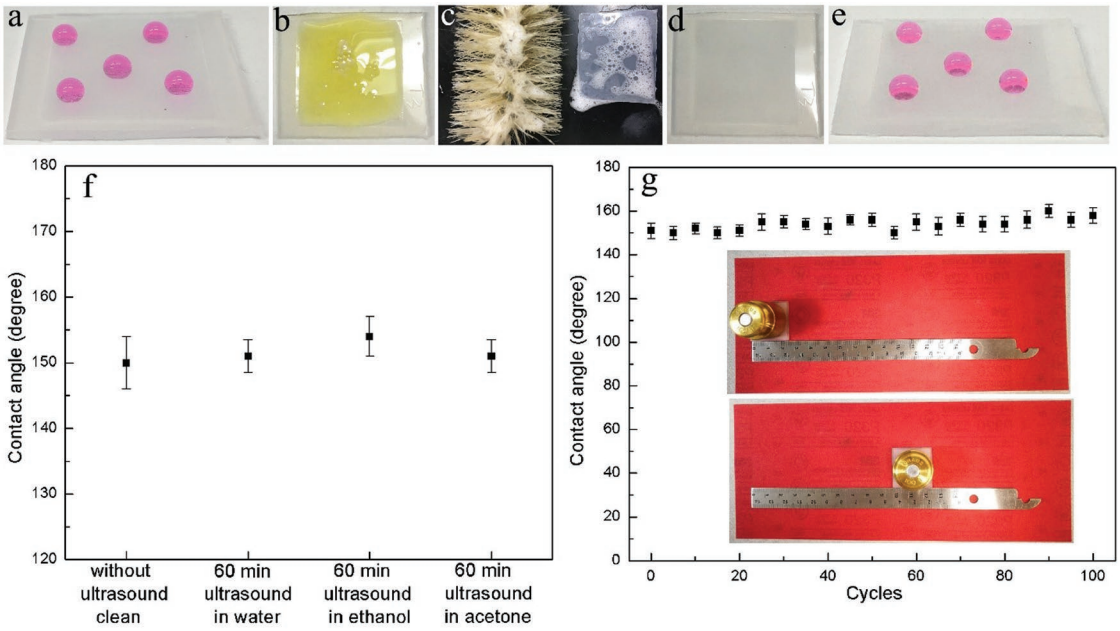

Figure 6. a–e) Photos of thermal-imprinted PP samples (a) before washing with water droplets, (b) contaminating by pump oil, (c) washing by a lab brush with liquid soap, and after washing (d) without and (e) with water droplets. f) Contact angle of a PP sample before and after ultrasound cleaning in pure water, ethanol and acetone for 60 min. g) The changing of contact angle of a PP sample after mechanical abrasion by a sandpaper (total 100 cycles).

In this work, aqueous ethanol solution of stearic acid and xylene liquid were used to assist in the demolding process and to remove the PP particles remaining on the Ti mold surface, respectively. These two strategies guaranteed the repeatability of the Ti mold, and hence the excellent fidelity of the thermal-imprinted PP surfaces, as shown in Figures 1 and 2. Therefore, the fabricated PP samples exhibit uniform and constant superhydrophobicity that is independent from the number of times of thermal imprinting.

As the washable property and mechanical durability are critical for all of the SHSs practical applications,[1c,3a] we tested our PP samples by brush wash, ultrasound cleaning, and sandpaper abrasion. As shown in **Figure 6**a–e, our thermal imprinted PP samples remain superhydrophobic after contamination by pump oil (Figure 6b) and subsequent cleaning by brush wash with liquid soap (Figure 6c). In order to check the washability of the thermal imprinted PP SHSs further, we ultrasounded the PP samples in pure water, ethanol, and acetone for 60 min, respectively, and checked the contact angles after these cleaning. The experimental results before and after the ultrasound cleaning are shown in Figure 6f. As can be seen, these ultrasound cleanings had no effect on the superhydrophobicity of the samples, the average contact angle keeps almost the same value of more than 150°. The sliding angle still keeps at about 4°–7°. As known, ultrasound cleaning in ethanol and acetone is an effective method to degrease and to clean surfaces deeply.[16] The PP SHSs fabricated here by our thermal imprinting method exhibits outstanding tolerance to the ultrasound cleaning either in ethanol or acetone, which is a breakthrough for their practical applications. The changing of contact angle of a PP sample after mechanical abrasion by sandpaper (grit no. 320) is shown in Figure 6g. In one abrasion cycle, the thermal imprinted PP surface with a weight of 100 g was placed face-down to a sandpaper and moved for 10 cm along the ruler; and then the sample was rotated by 90° (face to the sandpaper) and moved for 10 cm along the ruler (inset of Figure 6g), which guarantees the surface is abraded longitudinally and transversely in each cycle.[3a] As shown in Figure 6g, the static water contact angles after abrasion are between 147° and 163°, and the sliding angle keeps at ≈4°–7°, indicating that superhydrophobicity was not lost by even 100 cycles of mechanical abrasion.

The morphology changing of the PP surfaces during the brush wash, ultrasound cleaning, and sandpaper abrasion are checked by SEM and laser microscope. The results show that the brush wash and ultrasound cleaning almost did not change the morphologies of the PP surfaces. But the sandpaper abrasion process has changed the surface, as shown in Figure S12 of the Supporting Information. Although the abrasion process gradually destroyed the originally imprinted micro/nanostructures, the PP SHSs still possess rough surface even after 100 cycles of abrasion by a sandpaper (grit no. 320) with a weight of 100 g. The combination of the rough surface and the intrinsically nonpolar property of PP makes the thermal imprinted surface possesses superhydrophobicity even after serious abrasion. Due to no requiring chemical modification to low the surface energy, it is reasonable that the prepared PP SHSs withstand brush washing and ultrasound cleaning.

As known, SHSs rely on the nano/microscale surface textures and the modified nonpolar chemistry with lower surface energy (e.g., perfluorooctyltriethoxysilane).[1c,3a] This surface textures are highly susceptible to mechanical wear, and abrasion may also alter the surface chemistry.[1c,3a,17] Both processes can result in the relenting or loss of superhydrophobicity,

which makes mechanical durability a central concern for practical applications of SHSs. In addition, the adhesion between SH layers and underlying substrates is a key issue for the real using of SHSs.[1c,3a,5a] In our work, the nano/microscale textures are patterned directly on PP surfaces by thermal imprinting rather than by coating or painting. Therefore, the surface textures will never be peeled off during the cleaning or abrasion processes. Furthermore, our method does not require the chemical modification on PP surfaces, due to their intrinsically nonpolar property.[5a] As a result, our PP SHSs can tolerate brush washing, ultrasound cleaning, and sandpaper abrasion. For some practical application of SHSs, the contamination or fouling of the SHSs is unavoidable, such as in water–oil separation. The completely washable property and mechanical durability of our thermal imprinted PP SHSs can promote the moving of SHSs toward real-world applications.

Except for PP, the thermal imprinting method reported here can also be used to fabricate various plastic SHSs, such as polyethylene (PE), polytetrafluoroethylene (PTFE), and plastic materials for general household appliances. Figure S13 of the Supporting Information shows the water drop tests on the surfaces of PE, PTFE, and Sato toilet produced by American Standard with and without our thermal imprinting treatment. Obviously, the thermal imprinted areas exhibit excellent superhydrophobicity. As these plastics are broadly utilized in our household activities, this fast, easy, and cost-effective method of SHS replication has important application prospects.

3. Conclusion

We reported here a facile method to convert normal polymer surfaces to SHSs directly by a one-step thermal imprinting approach. Unlike other methods that use coatings of SH micro/nanostructures on surfaces, our nano- and microscale textures are formed directly on polymer surfaces by thermal imprinting processes, which eliminates the problem of adhesion of SH layers on various underlying substrates. By using an aqueous ethanol solution of stearic acid to assist in demolding process and xylene liquid to remove PP particle contamination on the Ti mold surface, our strategy guarantees the repeated use of the Ti mold. This thermal imprinting method can be used to fabricate SHSs of various thermoplastics that are broadly utilized in our daily life. The thermal imprinted plastic SHSs show superstrong resistance to harsh cleaning and mechanical abrasion, making it great for various SHS applications.

4. Experimental Section

For the mold, Ti plates of 25.4 × 25.4 × 1.3 mm that were purchased from GoodFellow were used. It is first degreased in acetone before fs laser processing. Stearic acid (98%), absolute ethanol, acetone, and PP sheets with thickness of 1.6 mm were purchased from Alfa Aesar. The p-xylene liquid (99.8%) was purchased from Fisher Chemical. All chemicals were analytical grade reagents and were used as received.

The Ti molds were processed by fs laser pulses to obtain a hierarchical micro- and nanoscale surface pattern. The technique is similar to that previously introduced.[9] In the experiments, an amplified Ti-sapphire laser system was used that generates 65 fs pulses with a central wavelength of 800 nm and at a pulse repetition rate of 1 kHz. The laser beam raster scans the Ti mold sample mounted on a computerized XY-translation stage. The pulse energy from the fs laser was about 1 mJ, and the linear velocity of the translation stage is 1 mm s^{-1}. The period between the adjacent scanning lines is 100 µm.

Thermal imprinting was performed on a hydraulic press with a heating plate. PP sheets were cut to ≈35 mm squared pieces and used as the imprinting material. Before the thermal imprinting, the produced Ti mold was immersed into an aqueous ethanol solution of stearic acid (0.1 M) for 3 min in order to form a layer of stearic acid, which will assist in the demolding process. During the thermal imprinting process, the Ti mold and PP sheet were first aligned and then placed on the heating plates and maintained at the setting temperatures (75–130 °C) for 3 min. Then pressure is increased to the setting pressures (5–20 MPa) gradually. After holding at this setting temperature and pressure for 3 min, the pressure was released and the PP sheet with Ti mold was removed from the heating plate. When the temperature of the PP sample cooled down to room temperature, the Ti mold was demolded from the PP sheet. Then the Ti mold was immersed into the ethanol solution of stearic acid again for the next round of thermal imprinting.

The surface structures of the Ti mold and PP samples were first analyzed by a confocal UV scanning laser microscope (KEYENCE, VK-9700). For a more detailed view, a scanning electron microscopy (SEM) was used to determine micro- and nanoscale surfaces. The SEM is a Zeiss-Auriga field emission SEM operating at an accelerating voltage of 5 kV. The surface contact angles, sliding angles, and contact angle hysteresis were measured by Kino SL200KB Contact Angle Meter. The diameter of the water drop was about 2.2 mm. The values of the contact angle were obtained automatically through the software Contact Angle Meter (Interfacial Chemistry Analysis System CAST 3.0). An ultrasonic cleaner (CREST, 275HTA) and sandpaper with grit no. of 320 (3M) were used to characterize the washability and mechanical durability of the PP SHSs, respectively.

Supporting Information

Supporting Information is available from the Wiley Online Library or from the author.

Acknowledgements

This work was supported by the Bill & Melinda Gates Foundation (OPP1119542), the US Army Research Office (W911NF-15-1-0319), and National Science Foundation (1701163 and 1722169) grants.

Conflict of Interest

The authors declare no conflict of interest.

Keywords

femtosecond laser processing, mechanical durability, polymer, superhydrophobic surfaces, thermal imprinting

Received: February 4, 2019
Revised: May 9, 2019
Published online:

[1] a) L. Feng, S. H. Li, Y. S. Li, H. J. Li, L. J. Zhang, J. Zhai, Y. L. Song, B. Q. Liu, L. Jiang, D. B. Zhu, *Adv. Mater.* **2002**, *14*, 1857; b) T. Y. Liu, C. J. Kim, *Science* **2014**, *346*, 1096; c) X. L. Tian, T. Verho, R. H. A. Ras, *Science* **2016**, *352*, 142; d) H. Liu, Y. D. Wang, J. Y. Huang, Z. Chen, G. Q. Chen, Y. K. Lai, *Adv. Funct. Mater.* **2018**, *28*, 1707415; e) M. J. Liu, S. T. Wang, L. Jiang, *Nat. Rev. Mater.* **2017**, *2*, 17036.

[2] a) G. Wen, Z. G. Guo, W. M. Liu, *Nanoscale* **2017**, *9*, 3338; b) C. Y. Huang, M. F. Lai, W. L. Liu, Z. H. Wei, *Adv. Funct. Mater.* **2015**, *25*, 2670.

[3] a) Y. Lu, S. Sathasivam, J. L. Song, C. R. Crick, C. J. Carmalt, I. P. Parkin, *Science* **2015**, *347*, 1132; b) J. C. Bird, R. Dhiman, H. M. Kwon, K. K. Varanasi, *Nature* **2013**, *503*, 385.

[4] a) Y. Oikawa, T. Saito, S. Yamada, M. Sugiya, H. Sawada, *ACS Appl. Mater. Interfaces* **2015**, *7*, 13782; b) Q. M. Pan, J. Liu, Q. Zhu, *ACS Appl. Mater. Interfaces* **2010**, *2*, 2026; c) I. Vilaro, J. L. Yague, S. Borros, *ACS Appl. Mater. Interfaces* **2017**, *9*, 1057; d) T. F. Xiang, Y. Han, Z. Q. Guo, R. Wang, S. L. Zheng, S. Li, C. Li, X. M. Dai, *ACS Sustainable Chem. Eng.* **2018**, *6*, 5598; e) F. R. Li, Z. R. Wang, S. C. Huang, Y. L. Pan, X. Z. Zhao, *Adv. Funct. Mater.* **2018**, *28*, 1706867; f) C. P. Ruan, K. L. Ai, X. B. Li, L. H. Lu, *Angew. Chem., Int. Ed.* **2014**, *53*, 5556; g) J. Song, H. Liu, M. X. Wan, Y. Zhu, L. Jiang, *J. Mater. Chem. A* **2013**, *1*, 1740; h) K. S. Liu, Y. Tian, L. Jiang, *Prog. Mater. Sci.* **2013**, *58*, 503; i) Z. B. Zhan, Z. H. Li, Z. Yu, S. Singh, C. L. Guo, *ACS Omega* **2018**, *3*, 17425.

[5] a) H. Y. Erbil, A. L. Demirel, Y. Avci, O. Mert, *Science* **2003**, *299*, 1377; b) T. Zhu, C. Cai, J. Guo, R. Wang, N. Zhao, J. Xu, *ACS Appl. Mater. Interfaces* **2017**, *9*, 10224; c) I. Hejazi, J. Seyfi, E. Hejazi, G. M. M. Sadeghi, S. H. Jafari, H. A. Khonakdar, *Colloids Surf., B* **2015**, *127*, 233.

[6] a) X. M. Hou, X. B. Wang, Q. S. Zhu, J. C. Bao, C. Mao, L. C. Jiang, J. A. Shen, *Colloids Surf., B* **2010**, *80*, 247; b) R. Rioboo, M. Voue, A. Vaillant, D. Seveno, J. Conti, A. I. Bondar, D. A. Ivanov, J. De Coninck, *Langmuir* **2008**, *24*, 9508.

[7] T. Zhu, C. Cai, C. T. Duan, S. Zhai, S. M. Liang, Y. Jin, N. Zhao, J. Xu, *ACS Appl. Mater. Interfaces* **2015**, *7*, 13996.

[8] a) J. Y. Sun, D. M. Wu, Y. Liu, Z. Z. Yang, P. S. Gou, *Polym. Eng. Sci.* **2018**, *58*, 952; b) D. M. Wu, J. Y. Sun, Y. Liu, Z. Z. Yang, H. Xu, X. T. Zheng, P. S. Gou, *Polym. Eng. Sci.* **2017**, *57*, 268; c) J. Y. Sun, H. W. Li, Y. Huang, X. T. Zheng, Y. Liu, J. Zhuang, D. M. Wu, *ACS Omega* **2019**, *4*, 2750; d) J. Y. Sun, D. M. Wu, Y. Liu, L. Dai, C. Jiang, *Adv. Polym. Technol.* **2018**, *37*, 1581; e) Z. B. Zhan, Y. Lei, *ACS Nano* **2014**, *8*, 3862; f) Z. B. Zhan, R. Xu, Y. Mi, H. P. Zhao, Y. Lei, *ACS Nano* **2015**, *9*, 4583; g) Y. J. Peng, H. X. Huang, H. Xie, *Sol. Energy Mater. Sol. Cells* **2017**, *171*, 98.

[9] a) D. W. Gong, J. Y. Long, P. X. Fan, D. F. Jiang, H. J. Zhang, M. L. Zhong, *Appl. Surf. Sci.* **2015**, *331*, 437; b) S. F. Toosi, S. Moradi, M. Ebrahimi, S. G. Hatzikiriakos, *Appl. Surf. Sci.* **2016**, *378*, 426; c) D. F. Jiang, P. X. Fan, D. W. Gong, J. Y. Long, H. J. Zhang, M. L. Zhong, *J. Mater. Process. Technol.* **2016**, *236*, 56; d) C. H. Lim, S. Y. Han, J. D. Eo, K. Kim, W. B. Kim, *J. Mech. Sci. Technol.* **2015**, *29*, 5107.

[10] a) J. L. Yong, S. C. Singh, Z. B. Zhan, F. Chen, C. L. Guo, *ACS Appl. Mater. Interfaces* **2019**, *11*, 8667; b) J. Guo, S. Yu, J. Li, Z. G. Guo, *Chem. Commun.* **2015**, *51*, 6493; c) J. L. Yong, S. C. Singh, Z. B. Zhan, F. Chen, C. L. Guo, *Langmuir* **2019**, *35*, 921; d) J. L. Yong, S. C. Singh, Z. B. Zhan, J. L. Huo, F. Chen, C. L. Guo, *ChemNanoMat* **2019**, *5*, 241.

[11] X. C. Shan, Y. C. Liu, Y. C. Lam, *Microsyst. Technol.* **2008**, *14*, 1055.

[12] a) A. Y. Vorobyev, C. L. Guo, *J. Appl. Phys.* **2010**, *108*, 123512; b) A. Y. Vorobyev, C. L. Guo, *J. Appl. Phys.* **2011**, *110*, 043102; c) B. Lam, C. L. Guo, *Light: Sci. Appl.* **2018**, *7*, 11.

[13] a) Y. L. Pan, B. Bhushan, X. Z. Zhao, *Beilstein J. Nanotechnol.* **2014**, *5*, 1042; b) L. C. Gao, T. J. McCarthy, *Langmuir* **2006**, *22*, 6234; c) J. T. Korhonen, T. Huhtamaki, O. Ikkala, R. H. A. Ras, *Langmuir* **2013**, *29*, 3858.

[14] S. G. Lee, H. S. Lim, D. Y. Lee, D. Kwak, K. Cho, *Adv. Funct. Mater.* **2013**, *23*, 547.

[15] M. J. Mayser, W. Barthlott, *Integr. Comp. Biol.* **2014**, *54*, 1001.

[16] Z. B. Zhan, F. Grote, Z. J. Wang, R. Xu, Y. Lei, *Adv. Energy Mater.* **2015**, *5*, 1501654.

[17] H. Zhou, H. X. Wang, H. T. Niu, Y. Zhao, Z. G. Xu, T. Lin, *Adv. Funct. Mater.* **2017**, *27*, 1604261.

